

Electronic Structure of Single-Atom Alloys and Its Impact on The Catalytic Activities

Ziyi Chen and Peng Zhang*

Cite This: *ACS Omega* 2022, 7, 1585–1594

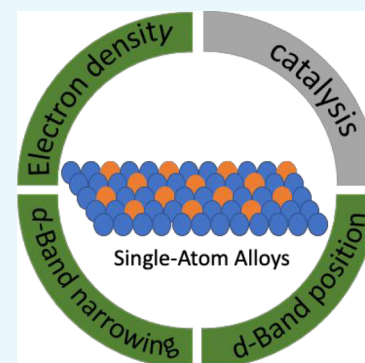
Read Online

ACCESS |

Metrics & More

Article Recommendations

ABSTRACT: Single-atom alloys (SAAs) are promising materials for heterogeneous catalysis due to their unique structure and electronic properties. SAAs have active sites narrowed down to the single-atom level, which combines the advantages of alloy materials and single-site catalysts. Given the unique structural feature of SAAs, their electronic properties can be more flexibly tailored than for their monometallic counterparts, which can be used to effectively control their catalytic activities. One interesting feature commonly observed for SAAs is the lower density of state (DOS) near the Fermi level than their bulk references. Comparing with results for their monometallic bulk reference, the most noticeable electronic property change in SAAs is the narrowing of the valence band, which gives them free-atom-like character. Moreover, the d-band position of both single atoms and their host metals can show a pronounced shift. These changes of electronic structure in SAAs could largely affect the adsorption behavior of adsorbates during the catalytic processes. Close examination of the relationship between electronic structure and catalytic activity can provide useful guidance for rational design of new catalysts with improved performance.



1. INTRODUCTION

Heterogeneous catalysts are one major category of catalysts, which have been widely used in chemical industry.¹ Metal-containing catalysts are an important part of heterogeneous catalysts. There are different ways to improve the catalytic activity of such materials. One way is to add different metals. Alloy metal catalysts have been studied widely, and they often exhibit better catalytic properties than their monometallic counterparts.² The addition of a second metal can tailor both the structural and electronic properties of materials, which can result in a change of their catalytic activity and selectivity. Another way is to reduce the size of active sites. Single-site catalysts are of great interest because active sites are narrowed down to single atoms, which maximize the atomic efficiency and provide uniform and well-defined active sites.² Single-atom alloys (SAAs) are one type of single-site catalysts, which consist of single metal atoms with high catalytic activity alloyed with less active metals. Therefore, SAAs combine the advantages of both traditional alloy materials and single-site catalysts.³ To avoid any confusion, it is important to distinguish SAAs and dual single-atom catalysts. They are both alloy catalysts with active sites at the atomic level. However, there exists only one type of active single atomic site in SAAs, and strong alloy interactions can present. If there exist two different types of metal in active single atomic sites, it is called a dual single-atom catalyst. The first SAA material was prepared by Sykes group, where isolated Pd atoms were dispersed on a clean Cu surface.⁴ Furthermore, the clearly defined active sites in SAAs help reduce the complexity of

systems, which can be beneficial to the understanding of the structure–property relationship.⁵ The challenge of studying SAAs is how to finely tune properties of such materials in order to obtain catalysts with high catalytic performance. Given the unique structure of SAAs, their electronic behavior of the catalysts can be changed, which can further affect their catalytic activities. Recent work on PtAu SAAs clearly showed that such catalysts can effectively avoid CO poisoning because of the reduced adsorption energy of CO on the SAA surface.⁶ Many studies revealed that the adsorption behavior on SAA surfaces is different from that on a pure metal surface.^{7–10} Therefore, a more complete understanding of the relationship between electronic behavior and catalytic properties can be helpful for the development of higher performance catalysts.

Many advanced techniques such as electron microscopy and X-ray spectroscopy have been applied to characterize SAAs. Here, we focus on understanding the electronic properties of SAAs from the perspectives of X-ray photoelectron spectroscopy (XPS), X-ray absorption near-edge structure (XANES), and density functional theory (DFT) calculations. XPS is a commonly used technique to probe the electronic structure

Received: October 29, 2021

Accepted: December 24, 2021

Published: January 6, 2022



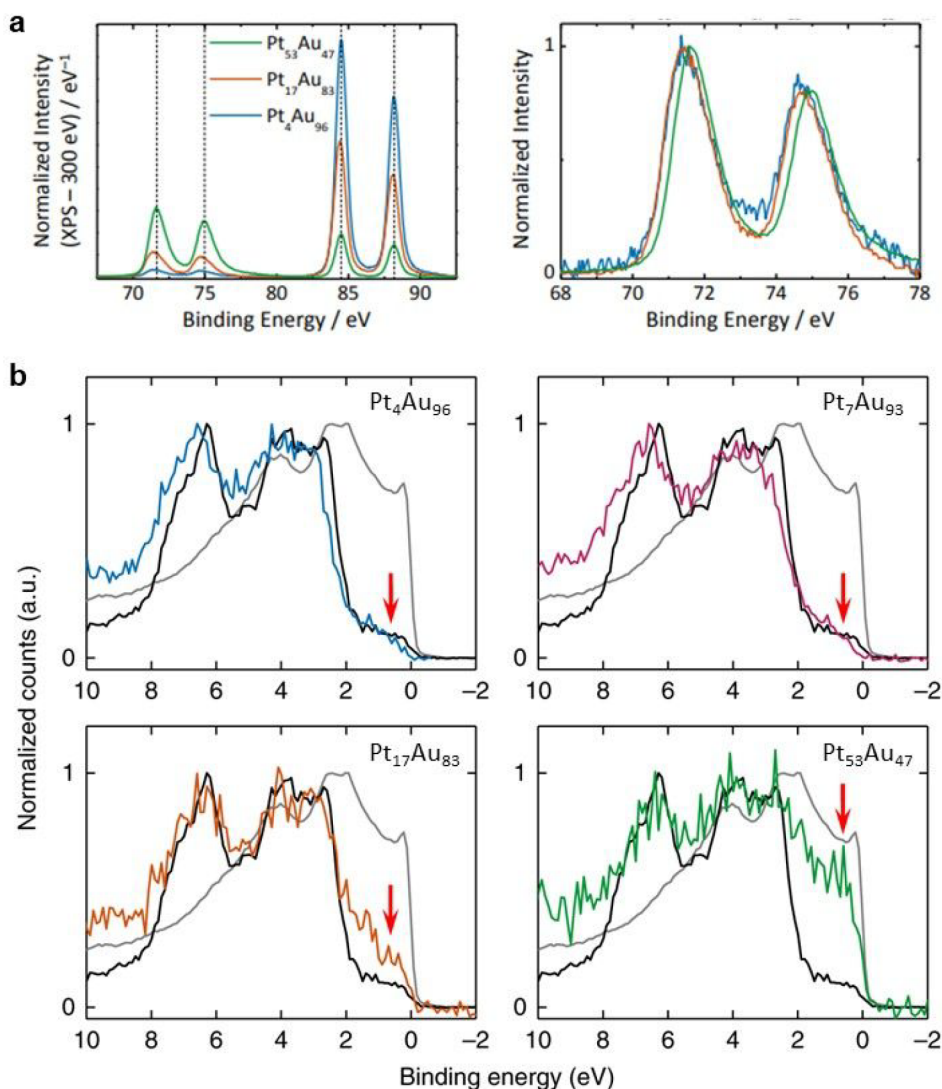


Figure 1. (a) XPS core-level spectra of PtAu nanoparticles and comparison of Pt 4f spectra of Pt₁₇Au₈₃, Pt₄Au₉₆, and Pt₅₃Au₄₇. (b) XPS valence band spectra of PtAu alloy samples compared with those of Pt (gray) and Au (black) foil references. Red arrows indicate the near-Fermi level region. Reproduced with permission from ref 6. Copyright 2018 Nature.

and density of states (DOS) of materials, which can reveal both core-level and valence band structure. In addition, in situ XPS is useful to study the electronic properties for SAA catalysts under reaction conditions.^{11,12} XPS could indicate the change of electronic properties of SAAs, but it can involve both initial- and final-state effects, which makes the interpretation of data complicated.¹³ The initial-state effect is associated with the intrinsic electronic structure, which can be affected by the metal interactions with ligands. The final-state effect is related to the process during measurements such as creation of a core hole and charge neutralization. If the charge neutralization cannot be done within a short time, the binding energy of XPS will shift.¹⁴ The determination of the origins of binding energy shift in XPS could be difficult. Hence, it requires other complementary techniques such as XANES. XANES is a region of X-ray absorption spectroscopy (XAS), and it corresponds to electronic transitions from core-level to unoccupied states.¹⁵ XANES has been successfully applied to the study of catalysts with dilute concentration such as Pd single-site catalysts,¹⁶ thiolate-protected SAAs nanoclusters.¹⁷ Analysis of XPS and XANES can provide information about changes on electron

density and the valence band, which is helpful for the understanding on their catalytic activities. Furthermore, DFT studies can offer in-depth information on how the electronic properties of SAAs can affect their catalytic performances. For example, DFT calculations have been shown to play an important role in the rational design of RhCu SAA catalysts.¹⁸ DFT calculations also have been successfully applied to reveal the origin of catalytic performance of PtCu SAAs in propane dehydrogenation reactions.¹⁹ In this review, the unique electronic structure of SAAs will be discussed from the perspective of electron density, valence band narrowing, and the d-band position. The emphasis is placed on how these electronic properties will impact the catalytic activities of SAAs.

2. ELECTRON DENSITY

Alloying single atoms with hosts can have impacts on electron density, which are typically observed by investigating their XPS spectra from both core-level and valence band. Elements in group 10 are often used as single atoms such as Pt and Pd. In the study of PtAu alloy nanoparticles with different ratios, it was found that the samples with low concentrations of Pt

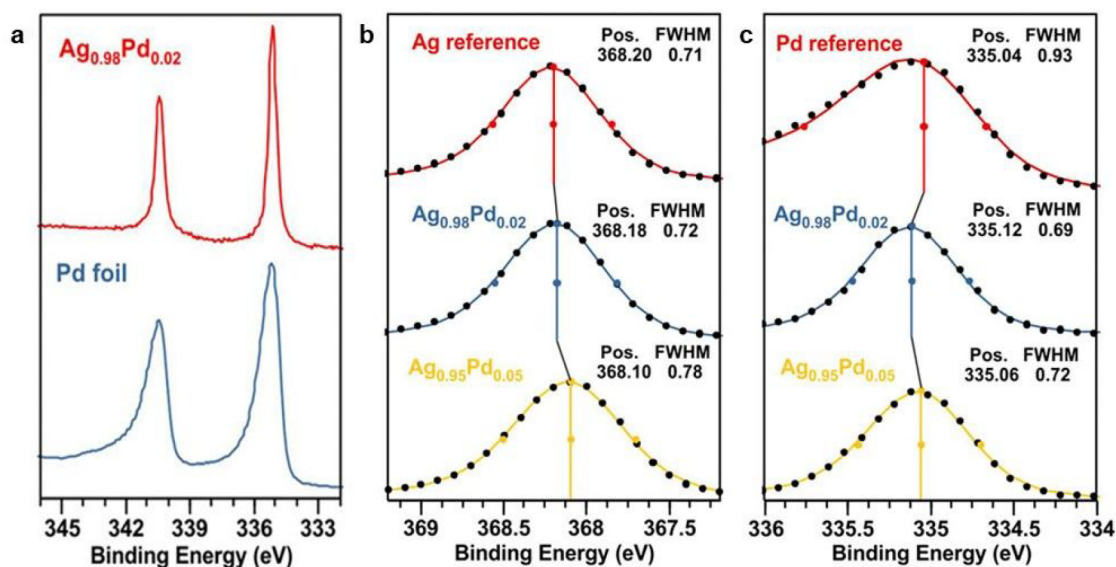


Figure 2. (a) Comparison of the Pd 3d of the $\text{Ag}_{0.98}\text{Pd}_{0.02}$ alloy with the polycrystalline Pd foil. (b) Comparison of the Ag $3d_{5/2}$ XPS spectra of $\text{Ag}_{0.98}\text{Pd}_{0.02}$ and $\text{Ag}_{0.95}\text{Pd}_{0.05}$ with pure Ag. (c) Comparison of the Pd $3d_{5/2}$ XPS spectra of $\text{Ag}_{0.98}\text{Pd}_{0.02}$ and $\text{Ag}_{0.95}\text{Pd}_{0.05}$ with pure Pd. Reproduced with permission from ref 20. Copyright 2021 American Institute of Physics.

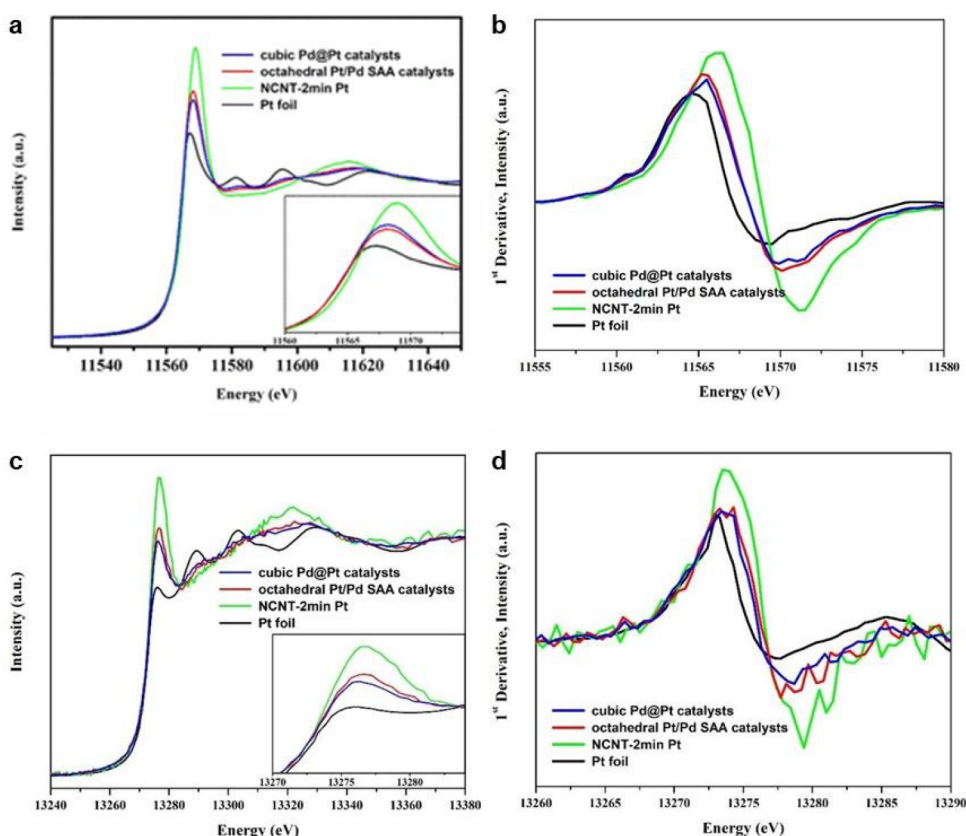


Figure 3. (a) Normalized XANES spectra at Pt L_3 edge. (b) First derivative of the XANES spectrum at Pt L_3 edge. (c) Normalized XANES spectra at Pt L_2 edge. (d) First derivative of the XANES spectrum at Pt L_2 edge. Reproduced with permission from ref 21. Copyright 2019 American Chemical Society.

($\text{Pt}_4\text{Au}_{96}$, $\text{Pt}_7\text{Au}_{93}$) are single-atom alloys.⁶ As shown in Figure 1a, the core-level Pt 4f XPS spectra of $\text{Pt}_4\text{Au}_{96}$ and $\text{Pt}_{17}\text{Au}_{83}$ exhibit negative shifts compared with results for more bulk-Pt-like $\text{Pt}_{53}\text{Au}_{47}$, indicating the change of electronic structure by the increase of Pt–Au bonding interactions. A more obvious change of electron density is shown in their valence band

spectra (Figure 1b). The DOS intensities of two SAA nanoparticles in the near-Fermi level region are lower than that of nanoparticles with higher Pt concentration. The spectra of these two samples have similar shapes to the spectrum of the Au foil reference. The intensity of the DOS near the Fermi level increases with the increase of Pt concentration. Therefore,

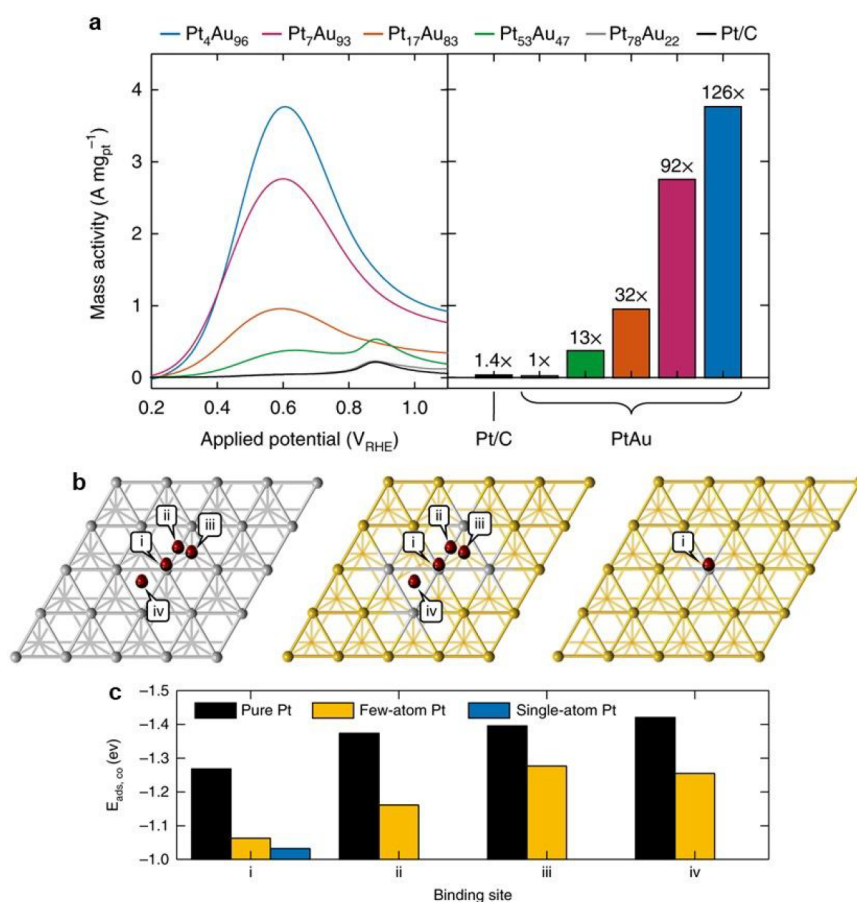


Figure 4. (a) Pt mass-normalized anodic sweeps obtained by cyclic voltammetry from PtAu nanoparticle catalysts in an electrolyte that contained 0.1 M concentrations of both HClO₄ and HCOOH, with the peak currents graphed for comparison (left). (b) Illustration of CO adsorption modes on model (111) lattices of pure (left), few atom (middle), and single atom (right). Pt surfaces show the apical (i), bridging (ii), hexagonal close-packed hollow (iii), and face-centered cubic hollow (iv) coordination sites. (c) Calculated adsorption energies for the indicated CO adsorption sites. Reproduced with permission from ref 6. Copyright 2018 Nature.

the valence band spectra of PtAu SAAs show mostly the Au characteristics.

The local DOS at the Fermi level can determine the degree of asymmetry of core-level XPS spectrum. More specifically, the asymmetry is caused by intrinsic energy losses resulting from interactions between core-level electrons and valence band electrons. For example, as shown in Figure 2a, the peak shape of the Pd 3d XPS spectrum for Ag_{0.98}Pd_{0.02} is symmetric, whereas the peak shape of bulk Pd XPS spectrum is asymmetric.²⁰ This is because AgPd SAAs have low DOS values around the Fermi level. Thus, in AgPd alloy nanoparticles, the Pd 4d-band is filled, so Ag 5s states are the primary states around the Fermi level, which reduces the chances of energy loss. Figure 2b shows a linear correlation between the energy shift of Ag 3d_{5/2} peak and the concentration of Pd. The Ag 3d_{5/2} peak shifts toward lower binding energy with the increase of concentration of Pd. This is the result of charge transfer from Ag 5s states to Pd 4d states. As the concentration of Pd increases, a more negative shift of the Ag 3d peak is observed because of additional hybridization effects. In this case, the shift of binding energy is mainly caused by the final-state effect. With the negative shift of binding energy, the Ag 3d peak width becomes broader. This broadening of Ag core-level peak in an alloy could be due to the Ag atoms in different coordination environments. Unlike Ag 3d spectra, there is no linear trend between the peak shift

and the concentration of Pd in Pd 3d XPS spectra (Figure 2c). Since the shape of the Pd 3d peak in the bulk is different from the peak shape of alloy nanoparticles, Ag_{0.98}Pd_{0.02} and Ag_{0.95}Pd_{0.05} are more comparable. The Pd 3d peak shows a negative shift as the Pd concentration increases.

Another essential tool to study the electron density of SAAs is XANES. Zhang et al. have successfully applied XANES spectra to study the electron density change of PtPd alloy.²¹ In Figure 3b,d, the first derivative spectra of XANES spectra for PtPd SAAs show a slight positive shift in the energy compared to spectra of the Pt foil. The Pt L-edge corresponds to the electron transitions from 2p to unoccupied 5d states. The white line intensity of PtPd SAAs is higher than that of the Pt foil, which indicates the highly unoccupied density of 5d states in the alloys. To quantitatively analyze the electron density, the occupancy of the Pt 5d states of the SAA and the Pt foil were determined. The Pt atoms in bimetallic nanoparticles exhibited a higher unoccupied density of the 5d states (0.8176) than the Pt atoms in the Pt foil (0.6754), indicating a higher interaction between Pt single atoms and the Pd surface in SAAs. In addition, the difference of the d-hole between the SAA and the Pt foil is 0.05 for h_{3/2} and 0.189 for h_{5/2}. Hence, the change of the number of d-hole for h_{5/2} is more significant than that for h_{3/2}.

The change of electronic structure of SAAs can have a significant impact on their catalytic activities because the

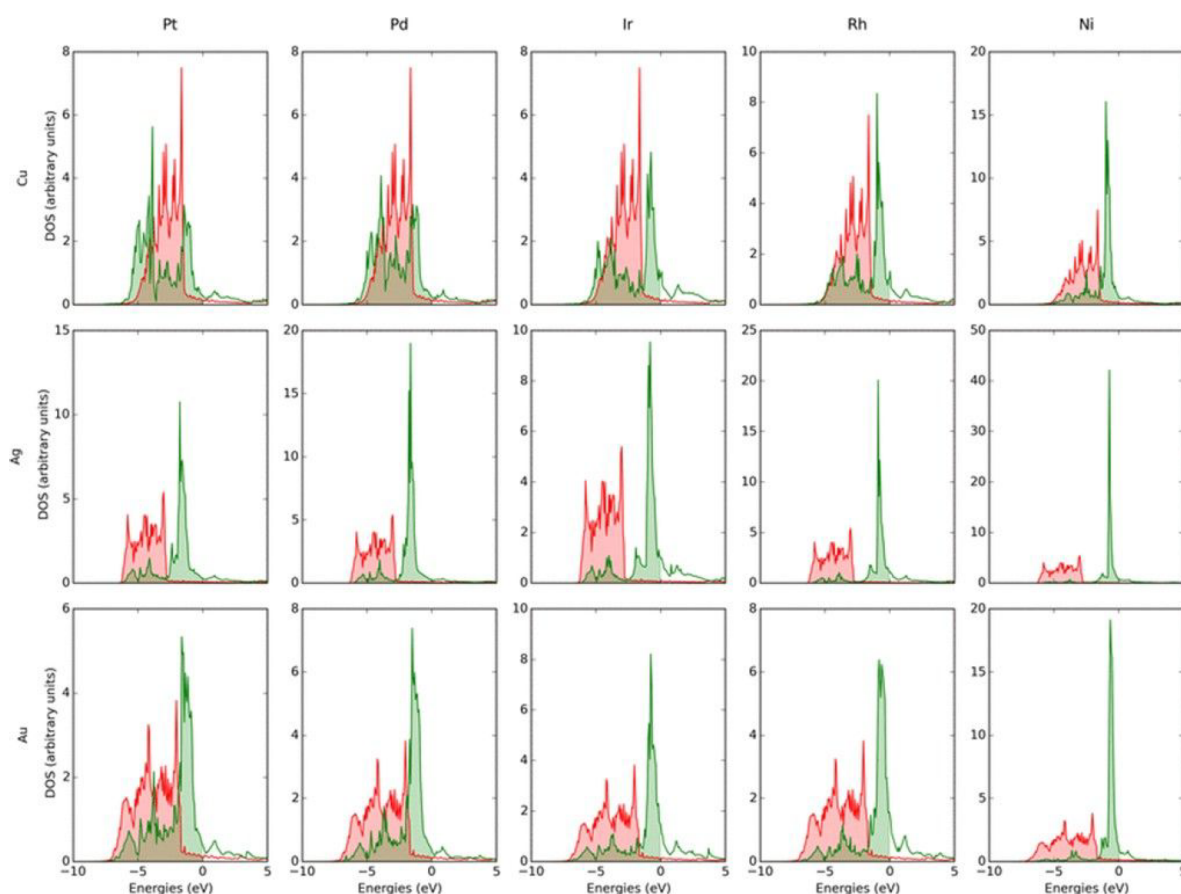


Figure 5. d-Band density of states for the fcc(111) single-atom alloy surfaces. The spectrum in red is that of the host metal atom, and that in green is that of the single atom in the alloy. The rows are host metals, and the columns are the single atoms. Reproduced with permission from ref 22. Copyright 2018 Springer Netherlands.

adsorption behavior of adsorbates can be influenced by SAAs. Depending on which reaction is studied, SAAs can enhance or weaken the interactions between adsorbates and SAA surfaces. The electron density is an important factor that can affect the adsorption processes. In the study of PtPd alloy, the single-atom Pt exhibits a higher density of unoccupied 5d orbitals compared with that of bulk Pt, which can facilitate the adsorptions of second and third H atoms on Pt.²¹ This improvement can help enhance the catalytic activity of the SAA for hydrogen evolution reaction, because the high H coverage on one Pt atom can facilitate the formation of H₂. On the other hand, the single Pt atoms in alloys can reduce the binding energy of OH on surface Pt atoms, which can increase the activity of the SAA for the oxygen reduction reaction as the rate-determining step is the desorption of OH. Thus, the same catalysts can have different functions depending on the reaction mechanisms. Furthermore, the durability of the PtPd catalysts is better than that of pure Pt catalysts because of the strong interaction between Pt atoms and Pd surface, which can enhance the stability.

In the design of a catalyst for a reaction that involves CO, the poisoning of catalysts is a problem. The single Pt atomic sites in PtAu alloys can avoid CO poisoning and improve the activity for oxidation of formic acid.⁶ In Figure 4a, the small peak between 0.8 and 1.0 eV indicates the adsorption of CO on the catalysts. This peak is absent in SAAs (Pt₄Au₉₆ and Pt₇Au₉₃), which suggests the resistance to CO poisoning. They both exhibit greater activity than commercial catalyst Pt/C. As

shown in Figure 4b,c, the adsorption behavior of CO at different sites was studied by DFT. It indicates that CO can adsorb on only the apical coordinate sites in the single-atom Pt surface, and the adsorption energy of CO at this site is -1.032 eV, which is smaller than the adsorption energies of CO on other surfaces. Thus, the single-atom Pt can weaken the adsorption of CO. In addition, the structure of the SAA makes this reaction favor the dehydrogenation mechanism to form CO₂ instead of the dehydration mechanism which can form CO to poison the catalyst. These PtAu alloys also show a good durability. The high catalytic activity can be retained even after 1500 rounds of potential cycling.

3. NARROWING EFFECT OF VALANCE BAND

The most interesting change of the electronic structure of SAAs would be the significant narrowing of the valence band compared with results for their bulk references. From the computational study of the d-band DOS of a single atom in different alloys (Figure 5), a sharp feature near the Fermi level was observed for most SAAs.²² The main reason for the sharp peak is that electron densities of host atoms and single atoms cannot mix effectively. Cu-based alloys show slightly different result from other SAAs. Their d-band DOS values of single atoms do not exhibit the sharp feature, which can be explained by compensating effect of compressive strain. For the Ag and Au-based alloys, the features of doped single atoms are similar to the free atom characteristics. When Ag atoms are host atoms, the dopant d-band peak is sharper than Au atoms as

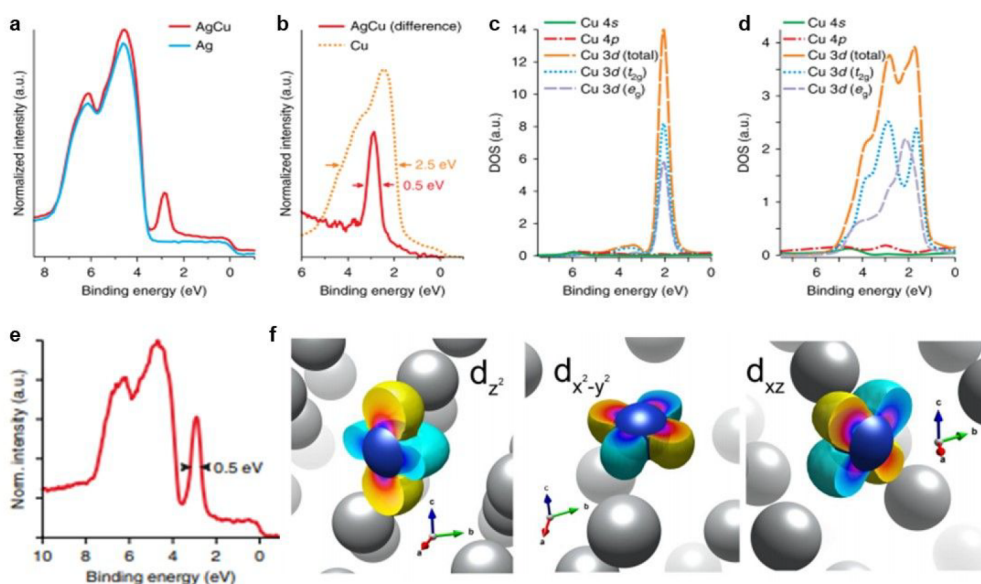


Figure 6. (a) Measured valence photoemission spectra ($h\nu = 150$ eV) of an AgCu alloy that contained 0.3 at. % Cu and metallic Ag. (b) Difference spectrum of AgCu and Ag, plotted with a Cu reference spectrum. (c) Calculated Cu-based projected DOS of $\text{Ag}_{31}\text{Cu}_1$. (d) Calculated Cu-based projected DOS of pure bulk Cu. (e) The valence photoemission spectrum of $\text{Ag}_{99.5}\text{Cu}_{0.5}$ measured under methanol re-forming conditions (0.5 mbar, 1:1 $\text{CH}_3\text{OH}:\text{H}_2\text{O}$, 300 °C). (f) Calculated Cu 3d wave functions of $\text{Ag}_{31}\text{Cu}_1$. Reproduced with permission from ref 12. Copyright 2018 Nature.

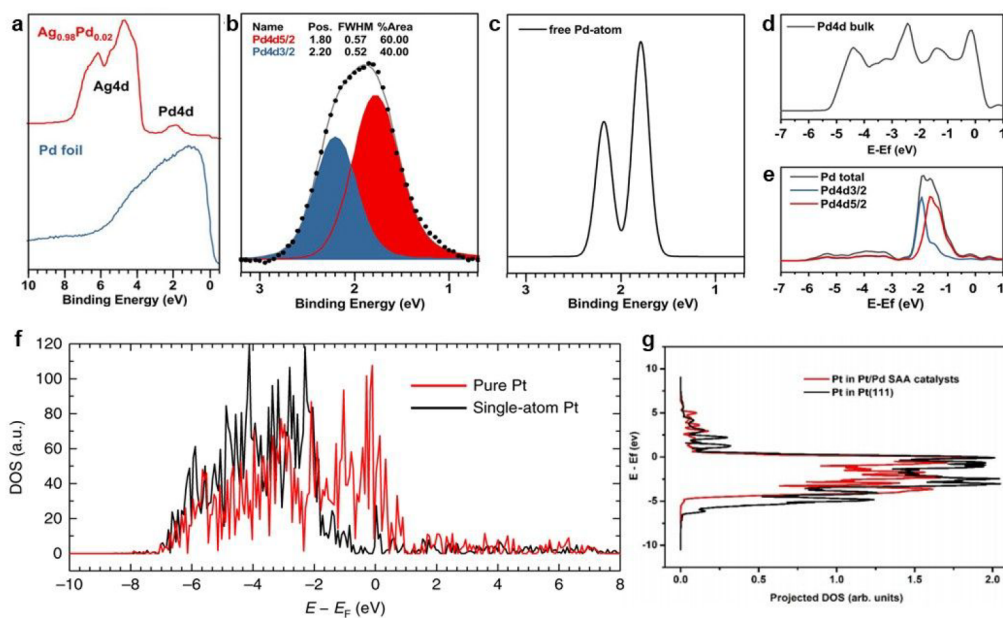


Figure 7. (a) Comparison of the valence states of $\text{Ag}_{0.98}\text{Pd}_{0.02}$ alloy with the polycrystalline Pd foil. (b) The two-peak fitting of Pd 4d valence states. (c) Calculated photoemission spectrum of a free Pd atom with spin-orbit splitting. (d) Pd 4d PDOS of bulk Pd. (e) Pd 4d PDOS of $\text{Ag}_{31}\text{Pd}_1$, including the spin-orbit splitting of Pd $4d_{3/2}$ and Pd $4d_{5/2}$. Reproduced with permission from ref 20. Copyright 2021 American Institute of Physics. (f) Calculated DFT DOS plots that correspond to the pure and single-atom Pt surfaces. Reproduced with permission from ref 6. Copyright 2018 Nature. (g) Calculated projected DOS of surface Pt atoms in Pt/Pd SAA catalysts and Pt(111) surface. Reproduced with permission from ref 21. Copyright 2019 American Chemical Society.

host due to the less electron density mixing between Ag and dopant atoms. Additionally, the d-bands of single atoms in Ag-based alloys appear at the energy closer to the Fermi level compared with the results for Au-based alloys. This observation can give an explanation to the higher reactivity of Ag-based alloys than Au-based alloys.

The sharp feature was also observed experimentally from XPS valence band. One good example is the AgCu alloy.¹² By

doping Ag with single Cu atoms, Greiner et al. found the significant narrowing of the Cu d-band compared with that of bulk Cu. The Cu d-bandwidth of the SAA is one-fifth of the bandwidth of bulk Cu (Figure 6b). This narrowing of the valence band is largely due to the energy mismatching between Cu 3d and Ag 4d states. Interestingly, this narrow d-band can be retained under the methanol re-forming condition, as shown in Figure 6e, which means the AgCu SAA catalyst can

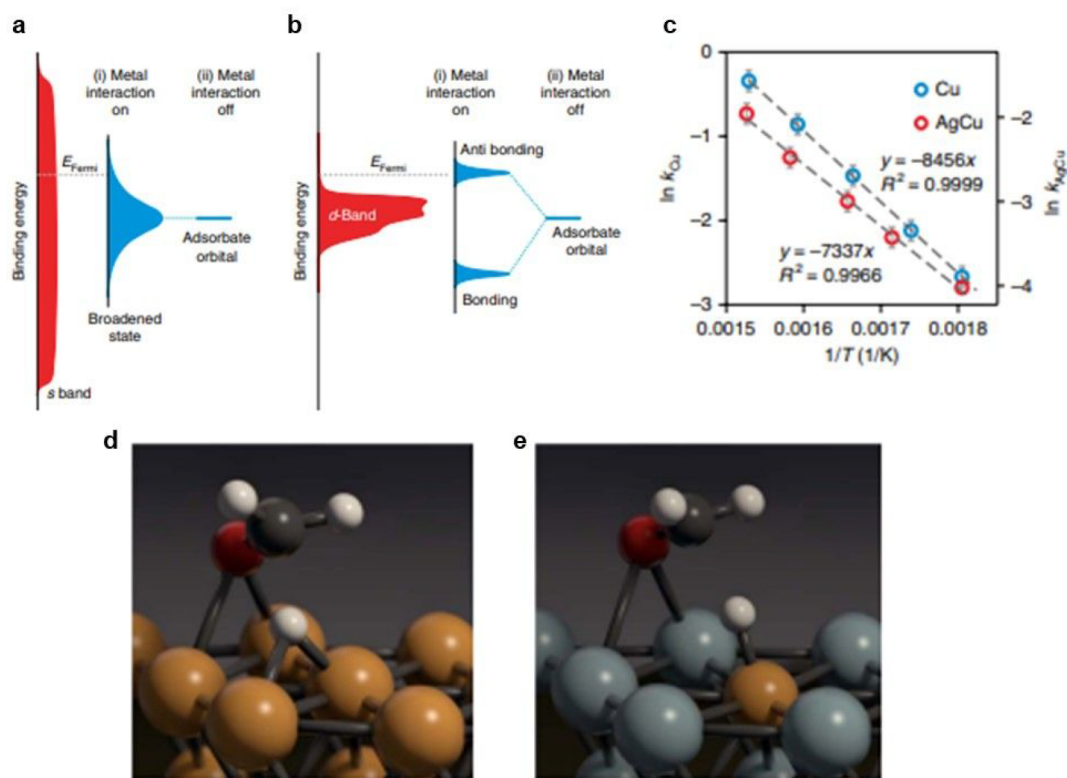


Figure 8. (a) Schematic DOS of an adsorbate bonding to a broad metal band. (b) Schematic DOS of an adsorbate bonding to a narrow metal band. (c) Arrhenius plots of H₂ production from Ag_{99.5}Cu_{0.5} and Cu. (d) Calculated structure of the transition states of the rate-limiting step for methanol re-forming on Cu. (e) Calculated structure of the rate-limiting step for methanol re-forming on Ag₃₁Cu₁. Reproduced with permission from ref 12. Copyright 2018 Nature.

maintain high activity in this reaction. Moreover, this narrow d-band can be reproduced by DOS calculations. The calculated the Cu projected DOS of Ag₃₁Cu and bulk Cu are shown in Figure 6c,d, respectively. The shape of the Cu 3d projected DOS in the alloy is symmetric, indicating Cu 3d is weakly hybridized with surrounding environment. In contrast, the Cu 3d line shape is irregular in bulk Cu, which reflects the strong hybridization between neighbouring atoms. In AgCu alloy, the e_g and t_{2g} states are overlapped, which implies that these two states are nearly degenerate. However, Figure 6d clearly shows that e_g and t_{2g} states are split due to strong hybridization. On the basis of both experimental and computational study, the Cu 3d states of the single Cu atom in the AgCu alloy have free-atom-like Cu d states. This character is clearly demonstrated in Figure 6f, which represents the spatial distribution and shape of Cu 3d wave functions.

This narrowing of the valence band was also observed in AgPd alloy nanoparticles.²⁰ The fwhm of Pd 4d in Ag_{0.98}Pd_{0.02} is 0.85 eV, which is narrower than the width of bulk Pd (Figure 7a). Pd 4d is well separated from Ag 4d, which means there exists no hybridization between these two states. Compared to the AgCu SAA results mentioned above, the peak width of Pd 4d is broader than the peak width of Cu 3d due to the spin-orbit splitting and the s–d coupling. Thus, the Pd 4d peak was fitted by two components with the area ratio constrained to 3:2 for d_{5/2}:d_{3/2} (Figure 7b). To verify if Pd atoms in Ag_{0.98}Pd_{0.02} have the free-atom-like electronic property, the photoemission signal of the free Pd atom was calculated (Figure 7c). It was found that the calculated splitting is 0.4 eV, which is consistent with the fitting results of Pd 4d in the XPS spectra. The

calculated projected DOS of the Pd 4d in bulk Pd shows a high DOS at the Fermi edge and is much broader than that calculated for Pd 4d of the SAA (Figure 7d,e). The narrowing effect is also shown in single-atom Pt in alloys. Figure 7 panels f and g demonstrate the calculated DOS of Pt in Au-based and Pd-based alloys.^{6,21} Pt atoms in the SAA exhibit a narrower bandwidth than bulk Pt. The narrowing effect is not as significant as the observation in AgCu and AgPd alloys. The possible reason for the less pronounced narrowing effect is that Pt is a 5d metal with more pronounced spin–orbit splitting than 3d and 4d metals.

The special narrowing effect of the valence band of single atoms can also affect the adsorption behavior. In the study of the AgCu alloy, the News–Anderson–Grimley model was applied to explain the adsorbate–surface bonding.¹² Figure 8 panels a and b show the model of adsorbates hybridized with broad and narrow metal valence bands, respectively. When adsorbates hybridized with broad valence bands, the adsorbate state becomes broader. However, when the metal valence band is narrow, the resulting adsorbate states can split into bonding and antibonding states. In general, the narrowing of the metal d-band can enhance the interaction strength. By examining the methanol re-forming, we found that the activation energy for AgCu alloy determined from Arrhenius plots (Figure 8c) is lower than that for bulk Cu. To further understand the improved catalytic activity, the geometries of the transition states were calculated. Since the rate-determine step is hydrogen abstraction from the methoxy group, the geometry of the abstracted hydrogen atom on bulk Cu and AgCu are shown in Figure 8d,e, respectively. The hydrogen atom

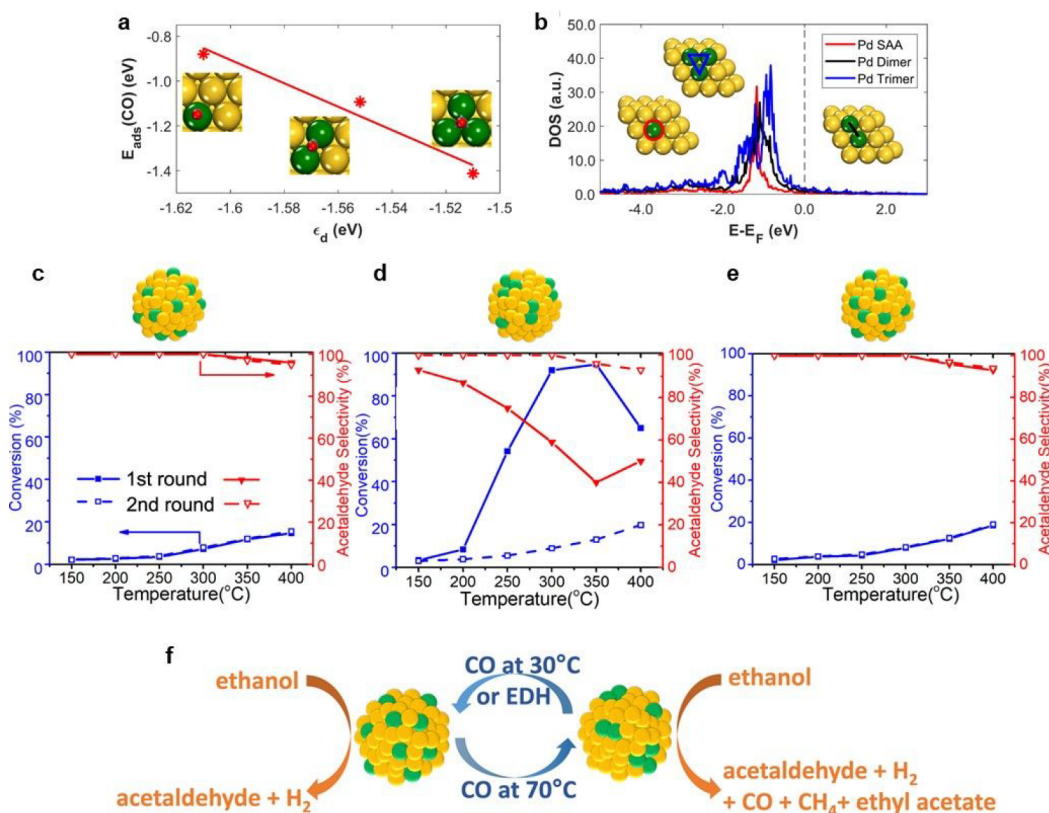


Figure 9. (a) Linear correlation between the CO adsorption energy and the d-band center of the d states of the Pd atoms that comprise the adsorption site. (b) d DOS plots in which the DOS are projected onto the same atoms. Au, Pd, C, and O atoms are shown in yellow, green, gray, and red, respectively. Structure and catalytic performance of a Pd_{0.02}Au_{0.98}/SiO₂ sample after (c) no CO treatment, (d) CO treatment at 30 °C for 30 min and then 70 °C for 30 min, which causes Pd to form clusters, and (e) CO treatment at 30 °C for 30 min, then 70 °C for 30 min, and then 30 °C for 1 h. (f) Schematic illustration showing how CO treatment can be used to change Pd from atoms to clusters and back, and the effect of these different active sites on the reaction pathway. Ethanol dehydrogenation reaction conditions: 300 mg of catalyst, 2% ethanol in helium, total flow rate 12 mL/min, GHSV = 2400 mL/(h·g_{cat}). Each temperature was held for 2 h. The solid line shows the first-round ethanol dehydrogenation reaction from 150 to 400 °C; the dotted line is the second round reaction. Each point is the average of data obtained during 2 h. Reproduced with permission from ref 24. Copyright 2021 Nature.

occupies a bridge site on the bulk Cu surface, whereas the hydrogen atom takes a nearly top-site position on the alloy surface, which indicates that the Cu–H bond in AgCu is stronger than the Cu–H bond in bulk Cu. However, an important thing that should be noticed is adsorbates can behave differently in various catalytic reactions. Thus, matching the adsorbate with a single-atom metal d-band is critical.

4. D-BAND POSITION AND ADSORPTION BEHAVIOR

Since d-band is involved in bond formation, studying the relationship between d-band position and adsorption behavior is important. Previous computational study shows that most SAAs exhibit lower binding energies with CO, and CO adsorption on the surface of SAAs could affect the structures such as segregation and aggregation.²³ Sykes group studied the interactions between CO and PdAu SAAs.²⁴ It was found that there is a linear correlation between the CO adsorption energy and the d-band center (Figure 9a). They examined single Pd atom, dimers, and trimers. The d-band center shifts to less negative values as the number of Pd atoms increases. As a result, the d DOS of dimers and trimers are closer to the Fermi level, as shown in Figure 9b. Because of this interaction behavior between CO and Pd, the structure of PdAu alloy can be tuned by inducing CO. The ethanol dehydrogenation was

selected as a probe reaction. Figure 9c shows the catalytic result of the Pd_{0.02}Au_{0.98} SAA without CO treatment, and it exhibits a low conversion rate but high selectivity to acetaldehyde and H₂. Then, the sample was cooled to 150 °C in ethanol flow, and the second round was performed while increasing the temperature from 150 to 400 °C. The result of the second round was the same as the first round, indicating the excellent stability of the SAA under ethanol dehydrogenation reaction conditions. In Figure 9d, the PdAu alloy was treated by first CO at 30 °C and then 70 °C. Under this reaction condition, the Pd cluster was presented, so the catalytic conversion rate became higher, but the selectivity decreased compared to the case for the alloy without CO treatment. After the sample was cooled and the second round was tested, the sample showed a low conversion rate and high selectivity, indicating that Pd clusters redispersed back to Pd atoms. In Figure 9e, the PdAu was treated with CO at 30 °C, 70 °C then 30 °C. The sample behaved similarly to the PdAu SAA. This result indicates that the single Pd atoms in PdAu alloy can aggregate to form Pd clusters at 70 °C and can redispersed back to single Pd atoms after subsequent 30 °C CO treatment. The experiment clearly demonstrated the dynamic structure change of PdAu alloy from the SAA to a Pd cluster structure under different CO treatment conditions, which can further control the catalytic performance (Figure 9f).

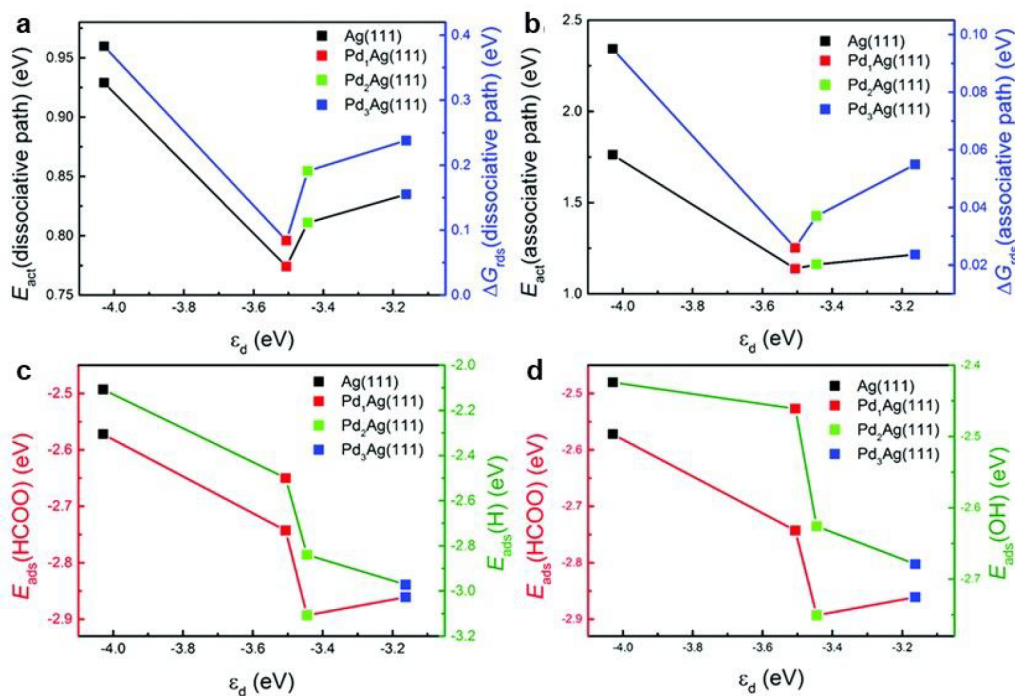


Figure 10. Relationship of the d-band center (ϵ_d) with the activation energy (E_{act}) of the HCOO decomposition reaction and the thermodynamic limiting energy (ΔG_{rds}) for (a) the direct dissociative path and (b) the direct associative path; the maximum adsorption energy (E_{ads}) of (c) HCOO and H intermediates and of (d) HCOO and OH intermediates for the Pd₁Ag(111) SAA, Pd₂Ag(111), and Pd₃Ag(111) alloy surfaces in reference to the Ag(111) surface. Reproduced with permission from ref 25. Copyright 2019 Royal Society of Chemistry.

The addition of single atoms into host metals could also affect the d-band position of host metals. The Ag-based single Pd atom alloy was studied for formate oxidation reaction.²⁵ In this case, the Pd₁Ag(111) SAA exhibits a narrow Pd d-band, which is about one-fifth the width of bulk Pd. The d-band center values of Ag(111), Pd₁Ag(111), Pd₂Ag(111), and Pd₃Ag(111) were compared to explore the impact on catalytic activity for formate oxidation. It was found that the d-band center shifts upward with the addition of Pd atoms into silver compared with results for the clean Ag(111) surface. This higher d-band center in alloy leads to a higher adsorption energy for HCOO, which can improve the catalytic performance. Among these three alloys, Pd₁Ag(111) shows the best catalytic performance because of a moderate d-band center value (Figure 10a,b). As shown in Figure 10c,d, the adsorption energy of H and OH on Pd₁Ag(111) is lower than those on other surfaces, which can promote H desorption in the direct dissociative path and the conversion of OH⁻ in the direct associative path. Therefore, Pd₁Ag(111) shows the lowest activation energy and thermodynamic limiting energy, suggesting the improvement of catalytic activity.

5. CONCLUSION

In conclusion, SAAs show unique electronic properties. They often exhibit lower DOS values near the Fermi level than their bulk references. The most interesting difference between the electronic structure of SAAs and their bulk counterparts is the significant narrowing of the valence band because of the ineffective mixing of valence bands between single atoms and hosts. Thus, these single atoms have an isolated electronic structure like a free atom. It was found that this narrowing effect is most significant for 3d SAAs. The d-band of SAAs is involved in the interactions between catalysts and adsorbed

species. Because of alloying and the special structure of SAAs, the d-band center of both single atoms and host metals can be altered, which could have effects on the adsorption strength. These changes on electronic structure of SAAs can ultimately have impacts on their catalytic activities. Alloying single atoms can enhance or weaken the adsorption strength of chemical species involved in the rate-determine step. Depending on the specific reaction studied, the design of SAAs could lead to a preferred adsorption behavior, either enhanced or weakened. The single atomic sites in alloys are desirable for catalysis because they provide active sites that are strong enough to adsorb reactants but also weak enough to desorb products. Meanwhile, adsorbates could affect the structure of SAAs, and thus it provides a new way to tune the structure of bimetallic materials. Overall, in-depth analysis of the electronic structure of SAAs associated with their catalytic activities provide valuable opportunities in understanding the structure–property relationship of these materials, which can guide the rational design of novel heterogeneous catalysts.

AUTHOR INFORMATION

Corresponding Author

Peng Zhang – Department of Chemistry, Dalhousie University, Halifax, NS B3H4R2, Canada;
Email: peng.zhang@dal.ca

Author

Ziyi Chen – Department of Chemistry, Dalhousie University, Halifax, NS B3H4R2, Canada

Complete contact information is available at:

<https://pubs.acs.org/10.1021/acsomega.1c06067>

Notes

The authors declare no competing financial interest.

Biographies

Ziyi Chen received her B.Sc. and M.Sc. from Dalhousie University. After completing her M.Sc., she worked as a research support staff member in the Zhang research group and is currently in this position. Her research focuses on X-ray absorption spectroscopy studies of Ag-based nanostructures and their catalytic and biomedical applications.

Peng Zhang received his B.Sc. and M.Sc. from Jilin University and Ph.D. from the University of Western Ontario. After spending two years at McGill University as an NSERC postdoctoral fellow, he joined Dalhousie University in 2005 as an assistant professor and currently is a full professor in the same university. His research focuses on the synchrotron X-ray spectroscopy studies of nanomaterials and their applications in catalysis and biomedicine.

ACKNOWLEDGMENTS

The authors are thankful for the financial support from NSERC Canada. This research used resources of the Advanced Photon Source, an Office of Science User Facility operated for the U.S. Department of Energy (DOE), Office of Science by Argonne National Laboratory, and was supported by the US DOE under Contract No. DE-AC02-06CH11357, and the Canadian Light Source (CLS) and its funding partners. The CLS was supported by the CFI, NSERC, NRC, CIHR, the University of Saskatchewan, the Government of Saskatchewan, and Western Economic Diversification Canada.

ABBREVIATIONS

SSAs, single-atom alloys; DOS, density of state; XPS, X-ray photoelectron spectroscopy; XANES, X-ray absorption near-edge structure; DFT, density function theory; XAS, X-ray absorption spectroscopy

REFERENCES

- Hannagan, R. T.; Giannakakis, G.; Flytzani-Stephanopoulos, M.; Sykes, E. C. H. Single-Atom Alloy Catalysis. *Chem. Rev.* **2020**, *120*, 12044–12088.
- Zhang, T.; Walsh, A. G.; Yu, J.; Zhang, P. Single-Atom Alloy Catalysts: Structural Analysis, Electronic Properties and Catalytic Activities. *Chem. Soc. Rev.* **2021**, *50*, 569–588.
- Mao, J.; Yin, J.; Pei, J.; Wang, D.; Li, Y. Single Atom Alloy: An Emerging Atomic Site Material for Catalytic Applications. *Nano Today* **2020**, *34*, 100917.
- Kyriakou, G.; Boucher, M. B.; Jewell, A. D.; Lewis, E. A.; Lawton, T. J.; Baber, A. E.; Tierney, H. L.; Flytzani-Stephanopoulos, M.; Sykes, E. C. H. Isolated Metal Atom Geometries as a Strategy for Selective Heterogeneous Hydrogenations. *Science* **2012**, *335*, 1209–1212.
- Darby, M. T.; Stamatakis, M.; Michaelides, A.; Sykes, E. C. H. Lonely Atoms with Special Gifts: Breaking Linear Scaling Relationships in Heterogeneous Catalysis with Single-Atom Alloys. *J. Phys. Chem. Lett.* **2018**, *9*, 5636–5646.
- Duchesne, P. N.; Li, Z. Y.; Deming, C. P.; Fung, V.; Zhao, X.; Yuan, J.; Regier, T.; Aldalbahi, A.; Almarhoon, Z.; Chen, S.; Jiang, D. en; Zheng, N.; Zhang, P. Golden Single-Atomic-Site Platinum Electrocatalysts. *Nat. Mater.* **2018**, *17*, 1033–1039.
- Schumann, J.; Bao, Y.; Hannagan, R. T.; Sykes, E. C. H.; Stamatakis, M.; Michaelides, A. Periodic Trends in Adsorption Energies around Single-Atom Alloy Active Sites. *J. Phys. Chem. Lett.* **2021**, *12*, 10060–10067.
- Chen, C. H.; Wu, D.; Li, Z.; Zhang, R.; Kuai, C. G.; Zhao, X. R.; Dong, C. K.; Qiao, S. Z.; Liu, H.; Du, X. W. Ruthenium-Based Single-Atom Alloy with High Electrocatalytic Activity for Hydrogen Evolution. *Adv. Energy Mater.* **2019**, *9*, 1803913.
- Zhang, X.; Cui, G.; Feng, H.; Chen, L.; Wang, H.; Wang, B.; Zhang, X.; Zheng, L.; Hong, S.; Wei, M. Platinum–Copper Single Atom Alloy Catalysts with High Performance towards Glycerol Hydrogenolysis. *Nat. Commun.* **2019**, *10*, 5812.
- Meng, G.; Sun, J.; Tao, L.; Ji, K.; Wang, P.; Wang, Y.; Sun, X.; Cui, T.; Du, S.; Chen, J.; Wang, D.; Li, Y. Ru1Con Single-Atom Alloy for Enhancing Fischer–Tropsch Synthesis. *ACS Catal.* **2021**, *11*, 1886–1896.
- Simonovis, J. P.; Hunt, A.; Waluyo, I. In Situ Ambient Pressure XPS Study of Pt/Cu(111) Single-Atom Alloy in Catalytically Relevant Reaction Conditions. *J. Phys. D: Appl. Phys.* **2021**, *54*, 194004.
- Greiner, M. T.; Jones, T. E.; Beeg, S.; Zwiener, L.; Scherzer, M.; Girgsdies, F.; Piccinin, S.; Armbrüster, M.; Knop-Gericke, A.; Schlögl, R. Free-Atom-like d States in Single-Atom Alloy Catalysts. *Nat. Chem.* **2018**, *10*, 1008–1015.
- Mason, M. G. Electronic Structure of Supported Small Metal Clusters. *Phys. Rev. B* **1983**, *27*, 748–762.
- Yang, D. Q.; Sacher, E. Initial- and Final-State Effects on Metal Cluster/Substrate Interactions, as Determined by XPS: Copper Clusters on Dow Cyclotene and Highly Oriented Pyrolytic Graphite. *Appl. Surf. Sci.* **2002**, *195*, 187–195.
- Zhang, T.; Chen, Z.; Walsh, A. G.; Li, Y.; Zhang, P. Single-Atom Catalysts Supported by Crystalline Porous Materials: Views from the Inside. *Adv. Mater.* **2020**, *32*, 2002910.
- Liu, P.; Zhao, Y.; Qin, R.; Mo, S.; Chen, G.; Gu, L.; Chevrier, D. M.; Zhang, P.; Guo, Q.; Zang, D.; Wu, B.; Fu, G.; Zheng, N. Catalysis: Photochemical Route for Synthesizing Atomically Dispersed Palladium Catalysts. *Science* **2016**, *352*, 797–801.
- Walsh, A. G.; Zhang, P. Thiolate-Protected Single-Atom Alloy Nanoclusters: Correlation between Electronic Properties and Catalytic Activities. *Adv. Mater. Interfaces* **2021**, *8*, 2001342.
- Hannagan, R. T.; Giannakakis, G.; Réocreux, R.; Schumann, J.; Finzel, J.; Wang, Y.; Michaelides, A.; Deshlahra, P.; Christopher, P.; Flytzani-Stephanopoulos, M.; Stamatakis, M.; Sykes, E. C. H. First-Principles Design of a Single-Atom-Alloy Propane Dehydrogenation Catalyst. *Science* **2021**, *372*, 1444–1447.
- Sun, S.; Sun, G.; Pei, C.; Zhao, Z. J.; Gong, J. Origin of Performances of Pt/Cu Single-Atom Alloy Catalysts for Propane Dehydrogenation. *J. Phys. Chem. C* **2021**, *125*, 18708–18716.
- Hartwig, C.; Schweinar, K.; Jones, T. E.; Beeg, S.; Schmidt, F.-P.; Schlögl, R.; Greiner, M. Isolated Pd Atoms in a Silver Matrix: Spectroscopic and Chemical Properties. *J. Chem. Phys.* **2021**, *154*, 184703.
- Zhang, L.; Liu, H.; Liu, S.; Norouzi Banis, M.; Song, Z.; Li, J.; Yang, L.; Markiewicz, M.; Zhao, Y.; Li, R.; Zheng, M.; Ye, S.; Zhao, Z. J.; Botton, G. A.; Sun, X. Pt/Pd Single-Atom Alloys as Highly Active Electrochemical Catalysts and the Origin of Enhanced Activity. *ACS Catal.* **2019**, *9*, 9350–9358.
- Thirumalai, H.; Kitchin, J. R. Investigating the Reactivity of Single Atom Alloys Using Density Functional Theory. *Top. Catal.* **2018**, *61*, 462–474.
- Darby, M. T.; Sykes, E. C. H.; Michaelides, A.; Stamatakis, M. Carbon Monoxide Poisoning Resistance and Structural Stability of Single Atom Alloys. *Top. Catal.* **2018**, *61*, 428–438.
- Ouyang, M.; Papanikolaou, K. G.; Boubnov, A.; Hoffman, A. S.; Giannakakis, G.; Bare, S. R.; Stamatakis, M.; Flytzani-Stephanopoulos, M.; Sykes, E. C. H. Directing Reaction Pathways via In Situ Control of Active Site Geometries in PdAu Single-Atom Alloy Catalysts. *Nat. Commun.* **2021**, *12*, 1549.
- Zhang, N.; Chen, F.; Guo, L. Catalytic Activity of Palladium-Doped Silver Dilute Nanoalloys for Formate Oxidation from a Theoretical Perspective. *Phys. Chem. Chem. Phys.* **2019**, *21*, 22598–22610.